

Effect of interface magnetization depinning on the frequency shift of ferromagnetic and spin wave resonance in YIG/GGG films

Fanqing Lin(林凡庆), Shouheng Zhang(张守珩), Guoxia Zhao(赵国霞), Hongfei Li(李洪飞), Weihua Zong(宗卫华), Shandong Li(李山东)

Citation: Chin. Phys. B . 2020, 29(6): 067601 . **doi:** 10.1088/1674-1056/ab8dac
Journal homepage: http://cpb.iphy.ac.cn; http://iopscience.iop.org/cpb

What follows is a list of articles you may be interested in

Large tunable FMR frequency shift by magnetoelectric coupling in oblique-sputtered $Fe_{52.5}Co_{22.5}B_{25.0}$/PZN-PT multiferroic heterostructure

Zhi-Peng Shi(时志鹏), Xiao-Min Liu(刘晓敏), Shan-Dong Li(李山东)

Chin. Phys. B . 2017, 26(9): 097601 . **doi:** 10.1088/1674-1056/26/9/097601

Magnetic transition behavior of perovskite manganites $Nd_{0.5}Sr_{0.3}Ca_{0.2}MnO_3$ polycrystalline

Ru Xing(邢茹), Su-Lei Wan(万素磊), Wen-Qing Wang(王文清), Lin Zheng(郑琳), Xiang Jin(金香), Min Zhou(周敏), Yi Lu(鲁毅), Jian-Jun Zhao(赵建军)

Chin. Phys. B . 2016, 25(4): 047601 . **doi:** 10.1088/1674-1056/25/4/047601

Magnetic hysteresis, compensation behaviors, and phase diagrams of bilayer honeycomb lattices

Ersin Kantar

Chin. Phys. B . 2015, 24(10): 107501 . **doi:** 10.1088/1674-1056/24/10/107501

Monte Carlo study of the magnetic properties of spin liquid compound $NiGa_2S_4$

Zhang Kai-Cheng, Li Yong-Feng, Liu Yong, Chi Feng

Chin. Phys. B . 2014, 23(5): 057501 . **doi:** 10.1088/1674-1056/23/5/057501

Microwave reflection properties of planar anisotropy $Fe_{50}Ni_{50}$ powder/paraffin composites

Wei Jian-Qiang,Zhang Zhao-Qi,Han Rui,Wang Tao,Li Fa-Shen

Chin. Phys. B . 2012, 21(3): 037601 . **doi:** 10.1088/1674-1056/21/3/037601

Effect of interface magnetization depinning on the frequency shift of ferromagnetic and spin wave resonance in YIG/GGG films*

Fanqing Lin(林凡庆)[1], Shouheng Zhang(张守珩)[1], Guoxia Zhao(赵国霞)[1], Hongfei Li(李洪飞)[2], Weihua Zong(宗卫华)[2], and Shandong Li(李山东)[1,†]

[1] College of Physics, Center for Marine Observation and Communications, Qingdao University, Qingdao 266071, China
[2] School of Electronics and Information, Qingdao University, Qingdao 266071, China

(Received 30 March 2020; revised manuscript received 22 April 2020; accepted manuscript online 28 April 2020)

Nowadays the yttrium iron garnet ($Y_3Fe_5O_{12}$, YIG) films are widely used in the microwave and spin wave devices due to their low damping constant and long propagation distance for spin waves. However, the performances, especially the frequency stability, are seriously affected by the relaxation of the interface magnetic moments. In this study, the effect of out-of-plane magnetization depinning on the resonance frequency shift (Δf_r) was investigated for 3-μm YIG films grown on $Gd_3Ga_5O_{12}$ (GGG) (111) substrates by liquid-phase epitaxy. It is revealed that the ferromagnetic resonance (FMR) and spin wave propagation exhibit a very slow relaxation with relaxation time τ even longer than one hour under an out-of-plane external magnetic bias field. The Δf_r span of 15.15–24.70 MHz is observed in out-of-plane FMR and forward volume spin waves. Moreover, the Δf_r and τ depend on the magnetic field. The Δf_r can be attributed to that the magnetic moments break away from the pinning layer at the YIG/GGG interface. The thickness of the pinning layer is estimated to be about 9.48 nm to 15.46 nm according to the frequency shifting. These results indicate that Δf_r caused by the pinning layer should be addressed in the design of microwave and spin wave devices, especially in the transverse magnetic components.

Keywords: yttrium iron garnet (YIG), magnetization relaxation, ferromagnetic resonance, spin waves

PACS: 76.50.+g, 85.70.Ge, 75.10.Hk, 75.25.−j **DOI:** 10.1088/1674-1056/ab8dac

1. Introduction

Spin magnetic moments of the electrons in magnetic materials will be precessing around their equilibrium position in an external field with a ferromagnetic resonance (FMR) frequency. If the spin precessions are not uniform, the propagation of collective precessions in a ferromagnet forms spin waves (the magnons are the quanta of spin waves).[1,2] The conventional complementary metal–oxide–semiconductor (CMOS) based electronics can no longer meet the requirements of high processing speed, small size, and low power consumption, one of the alternative methods having the ability to satisfy the above requirements is magnonics.[3–10] The aim of magnonics is to use spin waves to transmit, store, and process the information.[11–17] By encoding the information into the electron spin-angular momentum instead of the electron charge, the data can be processed faster with lower-energy dissipation.[18–23] In out-of-plane magnetized ferromagnetic films, the excited spin waves are called forward volume spin waves (FVMSW), here the group velocity v_g and the wave vector k are parallel. Unlike the backward volume magnetostatic waves (BVMSW) and magnetostatic surface spin waves (MSSW) excited in an in-plane magnetized ferromagnetic film, the FVMSW is isotropic, thus, overcomes the limitations of anisotropy spin waves in in-plane magnetized ferromagnetic films.[24]

For practical devices, it is essential that spin waves have a long propagation distance. Yttrium iron garnet ($Y_3Fe_5O_{12}$, YIG) is a proverbial ferromagnetic insulator with uniquely low magnetic damping, and spin waves can propagate a long distance over several centimeters in it, so it is the best material for magnonic devices so far.[11,25] In recent years, high-quality YIG films with ultralow damping for magnonic devices have been grown on gadolinium gallium garnet ($Gd_3Ga_5O_{12}$, GGG) substrates by liquid phase epitaxy,[26] radio frequency magnetron sputtering,[27] or pulsed laser deposition.[28] After the preparation of high-quality YIG thin films, the FMR and spin wave propagation properties of the films have been extensively studied.[15,29] In addition, spin-related phenomena such as spin pumping effect,[30] spin Hall magnetoresistance,[31] and spin Seebeck effect[32–34] in YIG films have aroused great interest in research. Meanwhile, YIG-based magnonic devices such as phase shifters, logic gates, filters, and multiplexers have been investigated. Propagation of short-wavelength spin waves in YIG films and interfacial spin-torque excited exchange spin waves have also been studied.[23,35] Among all the researches above, the frequency stability of FMR and spin waves in YIG films under a constant external magnetic bias field is very important either in fundamental research or the device design. However, there are rare reports about the frequency stability due to the inhomogeneous magnetization of

*Project supported by the National Natural Science Foundation of China (Grant Nos. 11674187 and 51871127) and Technology on Electronic Test & Measurement Laboratory (Grant No. 6142001180103).

†Corresponding author. E-mail: lishd@qdu.edu.cn

© 2020 Chinese Physical Society and IOP Publishing Ltd

YIG films. In this study, for the first time, the serious influence of magnetization relaxation in the pinning layer on the out-of-plane magnetized FMR frequency f_r, the FVMSW frequency f_{FVMSW}, and relaxation time τ was investigated. The results show that the f_r and f_{FVMSW} reduce with time. The frequency shift Δf can be attributed to that the magnetic moments at the YIG/GGG interface break away from the pinning layer. This study will provide valuable guidance for the application of YIG in FMR and spin wave devices.

2. Material and methods

The 3-μm YIG films were grown on single-crystal GGG (111) substrates using liquid phase epitaxy. Two YIG films of different dimensions were used to measure FMR and spin waves, respectively. Sample 1 with dimension of 2.5 mm×2.5 mm was used to measure FMR. Sample 2, a long strip waveguide with dimension of 10 mm×0.8 mm, was used to measure the propagation of the spin waves. The edges of the waveguide were cut to a 45° angle to avoid the influence of reflected spin waves. The crystal structure of the YIG films was characterized by high-resolution x-ray diffraction (XRD). As shown in Fig. 1(a), the XRD θ–2θ scan shows clear (444) orientation of the YIG film and substrate, signifying that the YIG films are well epitaxially grown on GGG substrates. The in-plane and out-of-plane hysteresis loops of the YIG films were measured by vibrating sample magnetometer (VSM). As shown in Fig. 1(b), the coercivities of the samples are all about 2.5 Oe along in-plane and out-of-plane, which indicates that the damping constant of the samples is small. The experimental result shows that spin waves can propagate above 1 cm in these YIG films. As shown in Fig. 1(c), the out-of-plane saturation magnetic field of the YIG film is about 2000 Oe, so the external magnetic field should be larger than 2000 Oe for out-of-plane FMR and FVMSW measurement.

In the practical experiment, the magnetic moments will take a very long time (about 24 hours) to completely recover to the random dispersion state. However, in order to ensure the data reliability, the magnetic relaxation process should be measured in the same sample, whose initial state should have a random dispersion of magnetic moments. For doing so, an ultrasonic vibration method was adopted to drive the moments to quickly recover to the random dispersion state after a measurement under a large magnetic field. The effect of the ultrasonic time on the moment recover process was explored. It is revealed that an ultrasonic vibration of half an hour is sufficient to bring the YIG moments to random dispersion. Therefore, treating the sample by ultrasonic vibration for 30 min after a measurement was adopted in this study. In addition, in order to ensure a stable magnetic field, in this experiment, a high stable power supply was adopted with a magnetic field stability better than 1 mOe/h.

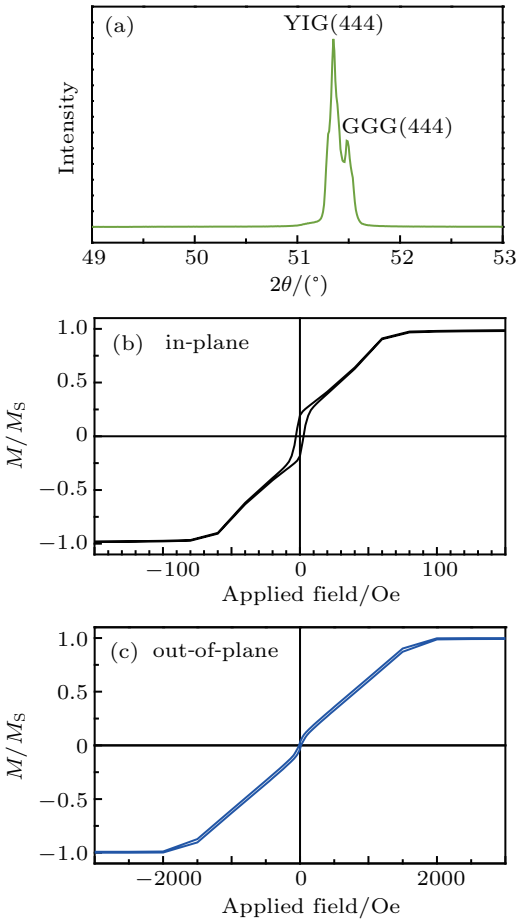


Fig. 1. (a) XRD θ–2θ scan of the (444) reflections from a YIG film grown on a GGG (111) substrate. Room-temperature in-plane (b) and out-of-plane (c) hysteresis loops of the YIG film.

A vector network analyzer (VNA, Agilent N5224 A) was employed to measure FMR spectra and spin wave transmission spectra using scattering parameter S_{21}. Two different measurement configurations were used to measure VNA-FMR and spin wave propagation, respectively. The FMR measurements were performed using a coplanar waveguide (CPW) with a signal line width of 300 μm and a distance of 220 μm between the signal line and the ground plane. The CPW was connected to the VNA ports, and the FMR spectra were measured by recording the S_{21} parameter as a function of frequency f and external magnetic field H_{ext}. Spin wave transmission spectra were measured by a YIG waveguide with input and output microwave microstrip antennas. The microwave signal through the input antenna generates an alternating magnetic field. The vertical component of the field perpendicular to the mean spins precession axis creates a torque that increases the precessional amplitude above the thermal level. Spins precessing under the antenna interact with the surrounding spins via exchange interaction, and when the field and frequency satisfy the appropriate conditions, the spin waves are propagating in the film. When the spin waves arrive at the output antenna, a microwave signal is induced through the inverse of the excitation process, and is detected by the VNA. By measuring S_{21} or S_{12} parameter, the spin wave transmission spectra in the sample can be

obtained. The variation of f_r and f_{FVMSW} with time was obtained by recording the S_{21} parameter in a time interval under a fixed external magnetic field.

3. Results and discussion

3.1. Relaxation of FMR frequency

In order to eliminate the influence of the microwave power on the FMR frequency and determine the optimum experimental condition, the S_{21} parameter was measured as a function of frequency f and microwave power P under a fixed out-of-plane external magnetic field H_{ext} of 4.03 kOe. Figure 2(a) shows the microwave power dependence of S_{21} at various P of −35 dBm, −30 dBm, −25 dBm, −20 dBm, −15 dBm, −10 dBm, −5 dBm, 0 dBm, 2.5 dBm, and 5 dBm. As illustrated, a large noise of the S_{21} parameters was observed at low power. However, a significant high power phenomenon occurs at high power. Figure 2(b) shows the FMR frequency, S_{21} intensity, and linewidth at half height at various microwave powers, in the case of $P \geqslant -10$ dBm, the FMR frequency moves toward the high frequency, the intensity becomes smaller, and the linewidth at half height increases. The results show that the power of −15 dBm is optimal since there is no high power phenomenon, and the noise of the S_{21} parameter is small. So the FMR spectra were measured under the microwave power of −15 dBm.

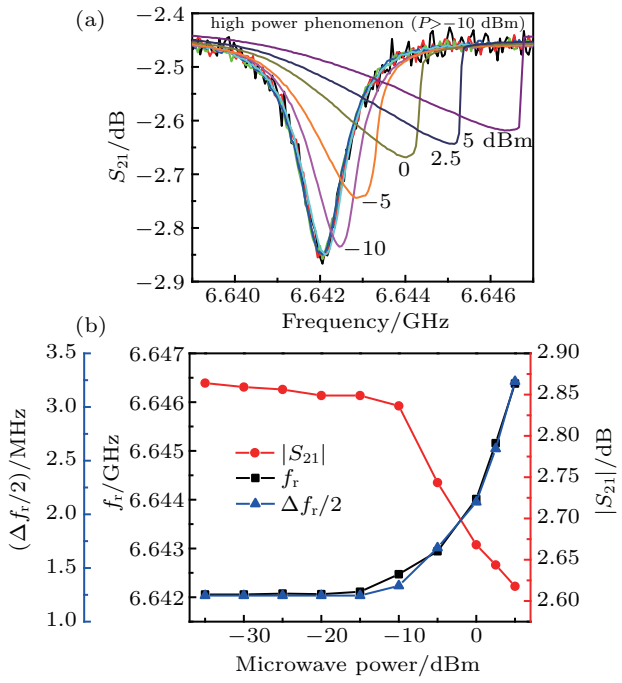


Fig. 2. (a) The S_{21} parameters showing FMR measured at out-of-plane external magnetic field $H_{ext} = 4.03$ kOe for different microwave powers: −35 dBm, −30 dBm, −25 dBm, −20 dBm, −15 dBm, −10 dBm, −5 dBm, 0 dBm, 2.5 dBm, 5 dBm. (b) FMR frequency f_r (black square), $|S_{21}|$ amplitude (red dot), and peak width at half height (blue triangle) as a function of the microwave power.

As described above, ultrasonic vibration was carried out for half an hour before the FMR measurement to eliminate the residual orientation of magnetic moments by the previous magnetization, and to return the sample to the state of random distribution of magnetic moments. The FMR measurement should be carried out immediately when H_{ext} reaches to the set value of the measuring field. Figure 3(a) shows the out-of-plane FMR frequency shift with time at various out-of-plane external bias fields under a microwave power of −15 dBm. The inset in Fig. 3(a) is a schematic of the FMR measurement configuration. A relaxation of FMR frequency f_r is observed when the external bias field is normal to the surface of the YIG film. It is revealed that a long time magnetization relaxation occurs in the YIG films, and the relaxation time is shortened with the increase of the magnetic field. For each applied field, f_r reduces rapidly at the beginning and tends to a stable value after a few minutes. The frequency shift Δf_r extracted from Fig. 3(a) is about 15.15 MHz to 24.70 MHz. For comparing the relaxation process, the frequency shift Δf_r was normalized using its maximum (Fig. 3(b)). As illustrated, it is obvious that the FMR frequency changes faster and the relaxation time is shortened with the increase of the bias magnetic field.

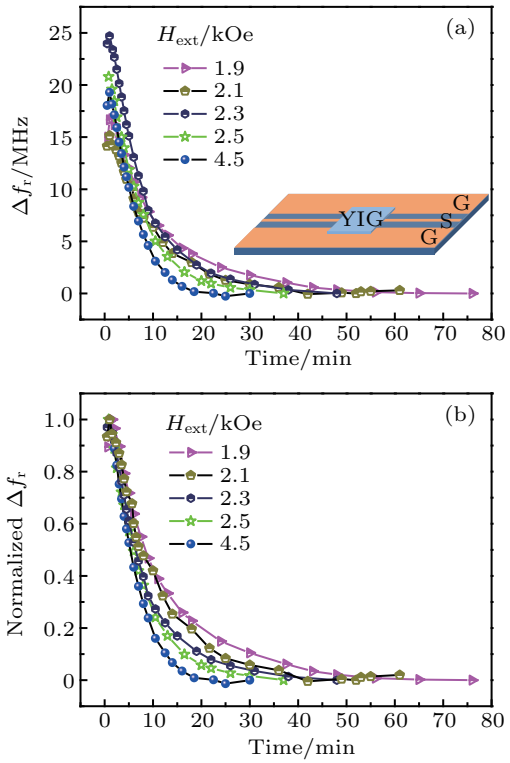


Fig. 3. (a) Time dependence of out-of-plane FMR frequency shift Δf_r under various applied external magnetic fields H_{ext}, (b) the normalized Δf_r–time curves.

The relationship between FMR frequency f_r and out-of-plane external magnetic field H_{ext} can be written approximately as

$$f_r = \frac{\gamma}{2\pi}(H_{ext} - 4\pi M_S), \tag{1}$$

where $\gamma/2\pi$ is the gyromagnetic ratio, and $4\pi M_S$ is the saturation magnetization. In Eq. (1), the effects of in-plane demagnetizing field and magnetocrystalline anisotropy are neglected,

and in general, the H_{ext} is greater than twice the saturation magnetization for saturating completely. Based on Eq. (1), a possible mechanism for the frequency shift of FMR and spin waves due to the relaxation of the pinning layer at the YIG/GGG interface is proposed (Fig. 4(a)). Without external magnetic field, the precession axis of the magnetic moments in the YIG film is in-plane. When a magnetic field is applied perpendicularly to the surface of the film, the magnetic moments located outside the pinning layer will immediately turn to the direction of the external field, while the magnetic moments in the pinning layer cannot turn to the external field immediately due to the YIG/GGG interface pinning. Since the magnetic moments in the pinning layer are not parallel to the magnetic field, the field exerts a torque $\boldsymbol{D} = \boldsymbol{\mu} \times \boldsymbol{H}_{ext}$ to them. The pinned moments will break away from the restriction of the GGG substrate under the torque, and gradually move towards the magnetic field direction. During this process, the magnetization along the normal direction increases gradually, equivalent to the increase of $4\pi M_S$ (Fig. 4(a) the middle column). Consequently, the FMR frequency is shifting to a lower frequency in a long relaxation time. On the other hand, as the external field increases, the torque becomes larger, the spin magnetic moments move to the external field in a shorter relaxation time. In order to substantiate our claim, the FMR frequency of in-plane magnetization as a function of time was measured. In contrast, the in-plane magnetized FMR frequency is nearly time independent, this verifies that the relaxation phenomenon is caused by the existence of the pinning layer.

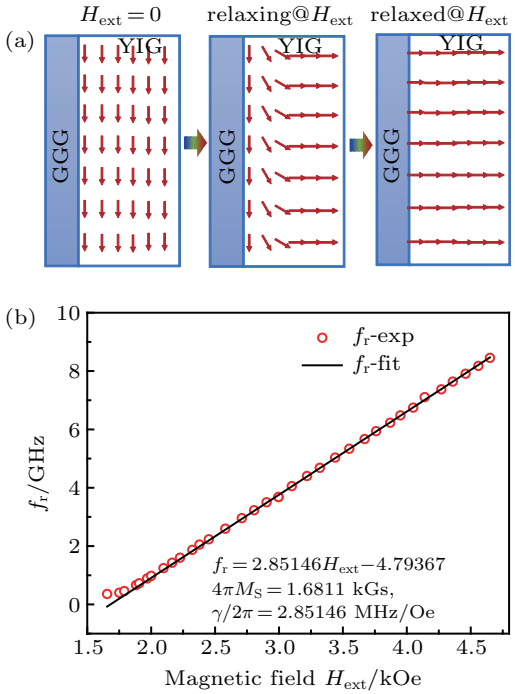


Fig. 4. (a) A schematic drawing for the principle of the relaxation of FMR and spin waves in the external field normal to the YIG film. (b) Out-of-plane FMR frequency f_r as a function of external magnetic field H_{ext}.

3.2. Pinning layer thickness estimation

In order to estimate the thickness of the pinning layer, the accurate gyromagnetic ratio $\gamma/2\pi$ and saturation magnetization $4\pi M_S$ of the YIG thin film were measured. The FMR spectra under various normal magnetic fields were recorded, and then the f_r–H_{ext} curve was fitted using Eq. (1). As shown in Fig. 4(b), $4\pi M_S = 1.6811$ kOe and $\gamma/2\pi = 2.85146$ MHz/Oe were obtained for the studied YIG film. If assuming only the pinning layer contributes to the frequency shift, the thickness of the pinning layer can be estimated by

$$d = d_0 \frac{-\Delta f_r}{\frac{\gamma}{2\pi} 4\pi M_S}, \tag{2}$$

where $d_0 = 3$ μm is the film thickness, and Δf_r is the FMR frequency shift before and after the relaxation. By using Eq. (2) and taking Δf_r in Fig. 3(a) into account, the thickness of the pinning layer of the YIG film is calculated to be about 9.48 nm to 15.46 nm. It should be noted that this value is the theoretical thickness of the pinning layer. In fact, there is a transition region between the pinning layer and the free layer, where spins gradually change from in-plane to out-of-plane.

3.3. Relaxation of FVMSW propagation frequency

The properties of spin waves depend on the strength of the dipolar and exchange interactions in the materials. As the wavelength of the spin wave becomes shorter, the angle between neighboring spins increases, and the energy of their exchange interaction increases too. Therefore, the long wavelength spin waves are dipole-dominated spin waves and the short wavelength spin waves are exchange-dominated spin waves. Generally speaking, the exchange-dominated spin waves have nanometer wavelength and propagate faster than the dipolar waves. However, the shorter waves are difficult to excite in practice and their propagation distance is very short as well. Therefore, for technical applications, the dipole-dominated spin waves are utilized mostly. A useful approximation to the dipole-dominated FVMSW dispersion relation is given by[36]

$$f_{FVMSW} = \sqrt{f_r \left[f_r + f_M \left(1 - \frac{1 - \exp(-kd_0)}{kd_0} \right) \right]}, \tag{3}$$

where $f_M = \gamma/2\pi \times 4\pi M_S$, k is the wave vector, and d_0 is the film thickness. It can be found that the FVMSW frequency, as the wave vector k tends to zero, tends to the out-of-plane FMR frequency f_r.

Figure 5(a) shows the normalized frequency shift of the FVMSW with time in various out-of-plane external magnetic fields. Similar to Fig. 3(b), the relaxation process of FVMSW frequency f_{FVMSW} is very similar with that of the FMR, where f_{FVMSW} also reduces with time, and it reduces rapidly at the

beginning and tends to a fixed value after a few minutes. Similarly, the stronger the H_{ext}, the faster the relaxation. This further proves that there is a pinning layer near the GGG substrate of the YIG thin film. Figure 5(b) shows the FVMSW spectra recorded at various time under a constant magnetic field H_{ext} of 4 kOe perpendicular to the waveguide. The FVMSW spectra move to a lower frequency as time increases.

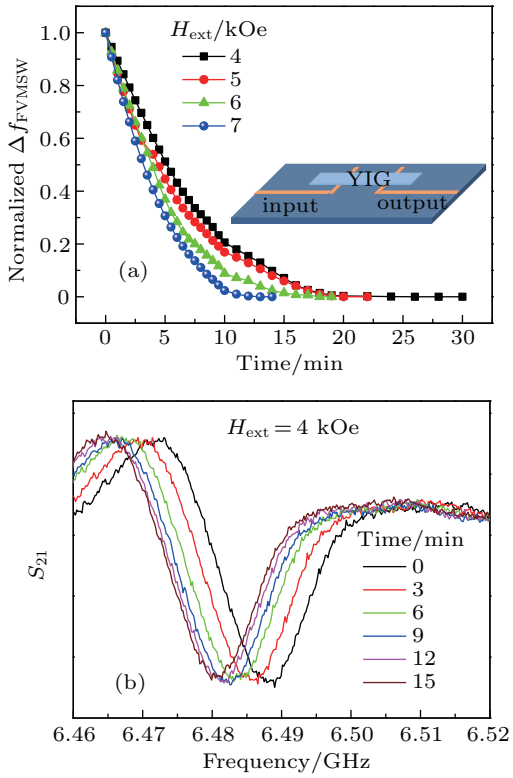


Fig. 5. (a) Normalized time dependence of FVMSW frequency shift Δf_{FVMSW} with various H_{ext}. The inset is a schematic of the FVMSW measurement configuration. (b) Part of the FVMSW transmission spectra (imaginary part of S_{21}) measured in out-of-plane external magnetic field $H_{ext} = 4$ kOe at various time.

In spin wave devices for signal transmission and processing, such as logic devices and microwave devices, the information carried by the spin waves is considered to be coded in terms of their phases. Therefore, accurate phase manipulation is important for spin wave devices. For standard methods of spin wave excitation and detection by means of microwave microstrip antennas or coplanar waveguides, the phase shift of the spin waves at a given magnetic field can be written as $\varphi(f) = k(f)x$, where f is the frequency of the spin waves and x is the distance between the input and output microstrip antennas. The variation of the phase shift is given by $\Delta\varphi(\Delta f) = \Delta k(\Delta f)x$, where Δk is the variation of the spin wave wavenumber. Δk is a function of the variation of spin wave frequency Δf, and this function can be theoretically calculated using the spin wave dispersion relation. For FVMSW, the relationship between Δf_{FVMSW} and Δk can be theoretically calculated by Eq. (3), and $\partial f_{FVMSW}/\partial k$ is the group velocity of FVMSW. In this experiment, the frequency shift Δf_{FVMSW} caused by magnetization relaxation is larger than 10 MHz. In many spin wave devices, the phase shift $\Delta\varphi$ caused by this frequency shift will exceed 2π, which will lead to a serious deterioration for the transmission and processing of the spin wave signal.

4. Conclusion

In summary, 3 μm-thick YIG films were grown on GGG (111) substrates by liquid-phase epitaxy. The relaxation of ferromagnetic resonance (f_r) and forward volume spin waves frequency (f_{FVMSW}) shift of vertically magnetized YIG films was studied. It is revealed that a long time relaxation of f_r and f_{FVMSW} occurs in the YIG films. The resonance frequency reduces rapidly at the beginning and then tends to a fixed value after a few minutes. Moreover, the stronger the magnetic field is, the shorter the relaxation time becomes. This can be explained by the magnetization relaxation of the pinning layer at the YIG/GGG interface. The phase shift caused by the frequency shift will adversely affect the vertical operation of spin wave devices. The thickness of the pinning layer is estimated to be about 9.48 nm to 15.46 nm.

References

[1] Chumak A V, Vasyuchka V I, Serga A A and Hillebrands B 2015 *Nat. Phys.* **11** 453
[2] Zhao X E, Hu Z Q, Yang Q, Peng B, Zhou Z Y and Liu M 2018 *Chin. Phys. B* **27** 97505
[3] Kruglyak V V, Demokritov S O and Grundler D 2010 *J. Phys. D: Appl. Phys.* **43** 264001
[4] Gu W J, Pan J and Hu J G 2012 *Acta Phys. Sin.* **61** 167501 (in Chinese)
[5] Davies C S, Francis A, Sadovnikov A V, Chertopalov S V, Bryan M T, Grishin S V, Allwood D A, Sharaevskii Y P, Nikitov S A and Kruglyak V V 2015 *Phys. Rev. B* **92** 020408
[6] Demidov V E, Urazhdin S, Zholud A, Sadovnikov A V, Slavin A N and Demokritov S O 2015 *Sci. Rep.* **5** 8578
[7] Sadovnikov A V, Beginin E N, Odincov S A, Sheshukova S E, Sharaevskii Y P, Stognij A I and Nikitov S A 2016 *Appl. Phys. Lett.* **108** 172411
[8] Shi Z P, Liu X M and Li S D 2017 *Chin. Phys. B* **26** 097601
[9] Sadovnikov A V, Grachev A A, Sheshukova S E, Sharaevskii Y P, Serdobintsev A A, Mitin D M and Nikitov S A 2018 *Phys. Rev. Lett.* **120** 257203
[10] Sadovnikov A V, Beginin E N, Sheshukova S E, Sharaevskii Y P, Stognij A I, Novitski N N, Sakharov V K, Khivintsev Y V and Nikitov S A 2019 *Phys. Rev. B* **99** 054424
[11] Serga A A, Chumak A V and Hillebrands B 2010 *J. Phys. D: Appl. Phys.* **43** 264002
[12] Lenk B, Ulrichs H, Garbs F and Munzenberg M 2011 *Phys. Rep.* **507** 107
[13] Nikitov S A, Kalyabin D V, Lisenkov I V, Slavin A, Barabanenkov Y N, Osokin S A, Sadovnikov A V, Beginin E N, Morozova M A, Sharaevsky Y P, Filimonov Y A, Khivintsev Y V, Vysotsky S L, Sakharov V K and Pavlov E S 2015 *Phys. Usp.* **58** 1002
[14] Chumak A V, Serga A A and Hillebrands B 2017 *J. Phys. D: Appl. Phys.* **50** 244001
[15] Qin H J, Hamalainen S J, Arjas K, Witteveen J and van Dijken S 2018 *Phys. Rev. B* **98** 224422
[16] Lv G, Zhang H and Hou Z W 2018 *Acta Phys. Sin.* **67** 177502 (in Chinese)
[17] Qiu Z Y and Hou D Z 2019 *Chin. Phys. B* **28** 88504
[18] Vogt K, Fradin F Y, Pearson J E, Sebastian T, Bader S D, Hillebrands B, Hoffmann A and Schultheiss H 2014 *Nat. Commun.* **5** 3727

[19] Chumak A V, Serga A A and Hillebrands B 2014 *Nat. Commun.* **5** 4700
[20] Wagner K, Kakay A, Schultheiss K, Henschke A, Sebastian T and Schultheiss H 2016 *Nat. Nanotechnol.* **11** 432
[21] Ganzhorn K, Klingler S, Wimmer T, Geprags S, Gross R, Huebl H and Goennenwein S T B 2016 *Appl. Phys. Lett.* **109** 022405
[22] Bang W, Lim J, Trossman J, Tsai C C and Ketterson J B 2018 *J. Magn. Magn. Mater.* **456** 241
[23] Klingler S, Amin V, Geprags S, Ganzhorn K, Maier-Flaig H, Althammer M, Huebl H, Gross R, McMichael R D, Stiles M D, Goennenwein S T B and Weiler M 2018 *Phys. Rev. Lett.* **120** 127201
[24] Klingler S, Pirro P, Brächer T, Leven B, Hillebrands B and Chumak A V 2015 *Appl. Phys. Lett.* **106** 212406
[25] Mihalceanu L, Vasyuchka V I, Bozhko D A, Langner T, Nechiporuk A Y, Romanyuk V F, Hillebrands B and Serga A A 2018 *Phys. Rev. B* **97** 214405
[26] Wang G, Liu H F, Wu H, Li X N, Qiu H C, Yang Y, Qu B J, Ren T L, Han X F, Zhang R Y and Wang H 2016 *Appl. Phys. Lett.* **109** 162405
[27] Gallagher J C, Yang A S, Brangham J T, Esser B D, White S P, Page M R, Meng K Y, Yu S S, Adur R, Ruane W, Dunsiger S R, McComb D W, Yang F Y and Hammel P C 2016 *Appl. Phys. Lett.* **109** 072401
[28] Howe B M, Emori S, Jeon H M, Oxholm T M, Jones J G, Mahalingam K, Zhuang Y, Sun N X and Brown G J 2015 *IEEE Magn. Lett.* **6** 3500504
[29] Lee S, Grudichak S, Sklenar J, Tsai C C, Jang M, Yang Q H, Zhang H W and Ketterson J B 2016 *J. Appl. Phys.* **120** 033905
[30] Kajiwara Y, Harii K, Takahashi S, Ohe J, Uchida K, Mizuguchi M, Umezawa H, Kawai H, Ando K, Takanashi K, Maekawa S and Saitoh E 2010 *Nature* **464** 262
[31] Nakayama H, Althammer M, Chen Y T, Uchida K, Kajiwara Y, Kikuchi D, Ohtani T, Geprags S, Opel M, Takahashi S, Gross R, Bauer G E W, Goennenwein S T B and Saitoh E 2013 *Phys. Rev. Lett.* **110** 206601
[32] Uchida K, Xiao J, Adachi H, Ohe J, Takahashi S, Ieda J, Ota T, Kajiwara Y, Umezawa H, Kawai H, Bauer G E W, Maekawa S and Saitoh E 2010 *Nat. Mater.* **9** 894
[33] Padron-Hernandez E, Azevedo A and Rezende S M 2011 *Phys. Rev. Lett.* **107** 197203
[34] Wang P, Zhou L F, Jiang S W, Luan Z Z, Shu D J, Ding H F and Wu D 2018 *Phys. Rev. Lett.* **120** 047201
[35] Liu C P, Chen J L, Liu T, Heimbach F, Yu H M, Xiao Y, Hu J F, Liu M C, Chang H C, Stueckler T, Tu S, Zhang Y G, Zhang Y, Gao P, Liao Z M, Yu D P, Xia K, Lei N, Zhao W S and Wu M Z 2018 *Nat. Commun.* **9** 738
[36] Damon R W and van de Vaart H 1965 *J. Appl. Phys.* **36** 3453